Nuclear Instruments and Methods in Physics Research B 324 (2014) 4–10

Contents lists available at ScienceDirect

Nuclear Instruments and Methods in Physics Research B

journal homepage: www.elsevier.com/locate/nimb

A laboratory X-ray microscopy setup using a field emission electron source and micro-structured reflection targets

P. Stahlhut [a,b,*], T. Ebensperger [a,c], S. Zabler [a,c], R. Hanke [a,c]

[a] Chair of X-ray Microscopy, University Wuerzburg, Josef-Martin-Weg 63, 97074 Wuerzburg, Germany
[b] Zentralinstitut für Neue Materialien und Prozesstechnik, Dr.-Mack-Str. 81, 90762 Fuerth, Germany
[c] Fraunhofer Development Center X-Ray Technology EZRT, Flugplatzstraße 75, 90768 Fuerth, Germany

ARTICLE INFO

Article history:
Received 11 June 2013
Received in revised form 6 December 2013
Available online 30 January 2014

Keywords:
Laboratory nano-CT
Reflection target
Geometric magnification

ABSTRACT

We present a computed tomography (CT) setup for materials characterization with significantly improved resolution as compared to state of the art mirco- or subμ-CT systems. The system presented here is composed of a customized JEOL JSM7100-F scanning electron microscope with a thermal field-emission electron source allowing to focus an intense electron beam onto specially designed micro-structured reflection target thereby further reducing the size of the X-ray source spot by reducing the electron interaction zone and thus reducing image blur at high magnifications.

With the proposed setup geometric magnifications up to $M = 1000$ and spatial resolutions down to 100 nm can be achieved. We also demonstrate the phase contrast capabilities of the setup.

1. Introduction

Ever since the groundwork on computed tomography by Cormack and Hounsfield, 3D X-ray imaging plays a significant role in clinical applications, non-destructive testing (NDT) and materials characterization [1]. Since these early years, great advances have been made with respect to acquisition time, spatial resolution and patient dose.

In contrast to clinical applications, dose uptake seldom plays a role in NDT and acquisition time is mostly relevant for the imaging of dynamic processes which require a certain time resolution per scan [2]. A state of the art X-ray micro-CT setup comprises a micro-focal transmission tube and is limited in spatial resolution to a few hundred nanometers whereby the thickness of the anode film acts both as a limit to resolution R and to flux, which is why long scan times are generally required for $R < 1$ μm [3]. The close proximity of the sample with respect to the source and the high heat load onto the latter make such experiments very vulnerable to errors caused by artificial motion of the focal spot. In order to overcome the limits of commercial systems, which have been at the best reported to resolve 250 nm line pairs, corresponding to approx. 400 nm FWHM focal spot size, SEM columns have been modified in order to realize (i) thinner transmission targets, or (ii) micro-structured reflection targets [4,5]. In fact, a variety of methods can be employed for X-ray nano-imaging. e.g., based on X-ray optics, viz. Fresnel zone plates can be resolved down to 30 nm resolution with $Cu_{K\alpha}$ photons [6]. At synchrotron beamlines it is further practical to focus X-rays with refractive elements or mirror-optics (Kirkpatrick-Baetz-systems) [7,8]. Using total X-ray reflection via waveguides or poly-capillaries [9] very high resolution down to 5 nm have been achieved recently in the range of 8 keV, yet these techniques will remain an exclusivity that can only be used at synchrotron light sources [10]. Laboratory setups with Fresnel zone plates have been realized but are very expensive and still limited in terms of energy range (8 keV) as well as in spatial resolution (approx. 50 nm in 2D imaging) [11].

Geometric magnification, on the other hand, achieves sub-micrometer resolution without any optical elements in the beam path, in analogy to early shadow microscopy [12]. The major advantage of using modified SEM stations for high-resolution X-ray imaging is that one can broad energy spectrum limited only by the acceleration voltage of the electron gun (30 kV), without filtering, whereas X-ray optics generally only perform for a small X-ray energy bandwidth. Given a very good mechanical stability and ultra-small electron focus, the spatial resolution in modified SEMs is basically defined by the lateral size of the anode material, be it a reflection or transmission target, both with their respective merits and flaws [13]. Here we present first results and tests on a recently developed laboratory X-ray microscope, which employs needle shaped reflection micro-targets of <100 nm tip radius [14].

2. General considerations

The geometric magnification M for a shadow microscope system is defined by focus-object distance z_1 and by the object-detector distance z_2 (cf. scheme in Fig. 1):

* Corresponding author at: Chair of X-ray Microscopy, University Wuerzburg, Josef-Martin-Weg 63, 97074 Wuerzburg, Germany. Tel.: +49 931 31 89240.
E-mail address: Philipp.Stahlhut@physik.uni-wuerzburg.de (P. Stahlhut).

0168-583X/$ - see front matter © 2014 Elsevier B.V. All rights reserved.
http://dx.doi.org/10.1016/j.nimb.2013.12.028

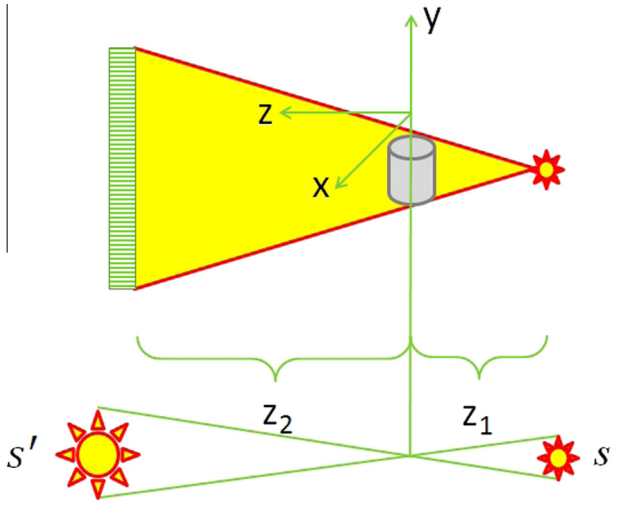

Fig. 1. The principle of geometric magnification, by using a pixilated detector. The projection of the source s on the imaging plane s', as well as the effective pixel size, both have an effect on the resolution. [13].

$$M = (z_1 + z_2)/z_1 \tag{1}$$

Given a pixelated detector, there are two limits to the spatial resolution of the system. (1) The detector point spread function which equals at least the physical pixel size P_P of the detector; and (2) The source size s. Using M to write P_P in the sample coordinate system leads to the sampling size P_S

$$P_P = M \cdot P_S \tag{2}$$

With few exceptions most high-resolution imaging systems comprise a focal spot that is significantly smaller than the detector pixel size, hence $s \ll P_P$. For $M > 2$, the source s is magnified geometrically onto the detector screen, where it causes a blurring s'

$$s' = s \cdot z_2/z_1 = s \cdot ((P_P/P_S) - 1) \tag{3}$$

For the present system we can safely assume a spot size $s < 100$ nm whereas the detector pixel size is $P_P = 55$ μm. Combining Eqs. (1)–(3) we obtain the spatial resolution of the displayed system P_{sys} in the sample coordinate system, which is mainly limited by, and only slightly smaller than the focal spot s

$$P_{sys} = s \cdot P_P/(s + P_P) \tag{4}$$

Note, that in the opposite case (synchrotron beamlines) where a large source (ca. 100 μm) is demagnified onto a very high-resolution detector (ca. 500 nm) the resolution limit is strictly defined by the latter which, in turn is limited by conversion of the X-rays into visible light (wavelength 500 nm).

3. Materials and methods

3.1. The experimental setup

The modified SEM is a JEOL JSM7100-F. The sample stage of the SEM was replaced by a piezo-driven dual-stage manipulator: one stage serves for the X-ray reflection target while the other one is the object stage (cf. Fig. 2). A 250 μm thick beryllium X-ray window was added to the system, allowing X-ray projections along a horizontal detector axis, which is 840 mm in total. This setup can thus be used for imaging magnifications up to 1000×.

The sample and target manipulators inside the SEM chamber are Klocke Nanotechnik GmbH (Aachen) piezo stages. They comprise three axes (x, y, z) for the X-ray needle nano-target, as well as two linear axis and one rotation for the sample. The setup and the stages are detailed in Fig. 3. This system allows high precision movement and stability for both target and object inside the vacuum chamber, which is necessary for this kind of application.

In order to realize an ultra-small X-ray focal spot we etched tungsten and molybdenum wires electrochemically in order to make a needle with a tip diameter below 100 nm. Using these reflection targets in a 90° geometry (the electron beam is vertical while the X-ray detector axis is horizontal), we can record ultra-high resolution images downstream of the Be-window (cf. Fig. 4). The electron column, when it operates at maximum power (320 nA filament current) delivers a very stable electron focus which has been found to be smaller than 10 nm, at an acceleration voltage of 30 kV.

For detecting the X-rays, we use a photon counting detector, i.e., a 300 μm thick Si-Medipix2 Hexa-chip MXR2 [15] with 768 × 512 pixels and 55 μm sampling. The performance of the Medipix-detector is similar to a deep depletion highly-cooled CCD camera. In fact such low-noise detectors are required because of the very long exposure times (some 10 min) which essentially result from the poor photon flux of the nano-source.

3.2. Micro-structured reflection target

The key to generate small X-ray focal spots is – in addition to a highly focused electron beam – the reduction of the physical size of the electron interaction zone inside the target material, from which the X-rays are emitted through Bremsstrahlung and fluorescence. For transmission targets this reduction is achieved by using very thin metal foils (<1 μm), e.g., through vapor deposition or sputtering of the exit window which is typically made of Be or Diamond [16]. The transmission version of such an ultra-microscope has the drawback that axial CT is very difficult to realize when the sample has to approach the window to a distance below 1 mm which is necessary for the high magnifications. In fact X-ray laminography is the preferred method to generate 3D data with such a setup. With a nano-reflection target, e.g. a very sharp metal needle, axial CT is no problem and can be performed even with focus-object distances well below 1 mm, provided that the sample is in vacuum.

We produce metallic needles from wires using electrochemical etching yielding tip diameters below 100 nm [17]. Therefore we use a 2 N sodium hydroxide solution as electrolyte to etch two electrodes of identical materials. These are 0.5 mm thick wires of tungsten or molybdenum. Then an AC voltage is applied for several minutes, whereby the etching process is mainly controlled by the bubble growth and movement along the tip and much less by gradient in the electrochemical potential.

During the first half of the AC voltage cycle metal oxides are dissolved at the tip (anode) and the bubble buoyancy carries them upwards, where they get partially reabsorbed on the wire (cathode) during the second half of the cycle. As a result the removal rate of the metal is a higher at the tip as shown in Fig. 5, and the tip is sharpened.

Both molybdenum and tungsten have electrochemical properties which make them good candidates for this kind of electrochemical AC etching. They are base metals and feature electrochemical standard potentials which facilitate the etching process (tungsten: −0.58 V, molybdenum: −0.20 V, both 298 K in water, against standard hydrogen electrode). The two metals furthermore feature very high melting points, which in combination with sufficient thermal conductivity are necessary for the stability of these small structures during electron bombardment. Both materials feature strong characteristic lines ($Mo_{K\alpha 1}$ = 17.48 keV and $W_{L\alpha 1}$ = 8.40 keV) [18] which lie within the emitted X-ray spectrum (0–30 keV).

The shape of the resulting tip is controlled via the AC frequency, and the voltage (peak-to-peak), as well as by the viscosity of the